VISUAL SNOW SYNDROME

A progress report specially prepared for

Visual Snow Initiative

April 2024

King's College LONDON

INTRODUCTION

We are delighted to present you with this update on Visual Snow Syndrome and Dr Puledda.

Research is core to King's, what we do, what we care about and how we educate. Our enquiry-driven research delivers transformative insights with the power to advance and accelerate global progress. Our academics work across disciplines and collaborate with partners so that our research changes practice and influences understanding at home and abroad. Here at King's, our researchers take world-leading ideas and turn them into life-changing impact.

Thanks to your support, Dr Francesca Puledda and her colleagues at the Institute of Psychiatry, Psychology & Neuroscience at King's are making significant strides in understanding Visual Snow Syndrome and its basis. In supporting this work, you are not only enabling a world-leading researcher in the area to reach significant research miletsones, but also impacting all those who currently live with Visual Snow Syndrome.

In this report we have included Dr Puledda's most recent success – a startling breakthrough into understanding the biological basis for Visual Snow Syndrome. You will find the full published paper announcing this discovery at the end of the report.

Your kind support and the partnership that we have established is prized both by Dr Puledda and the wider King's community. Thank you.

A NEW DISCOVERY

King's College LONDON
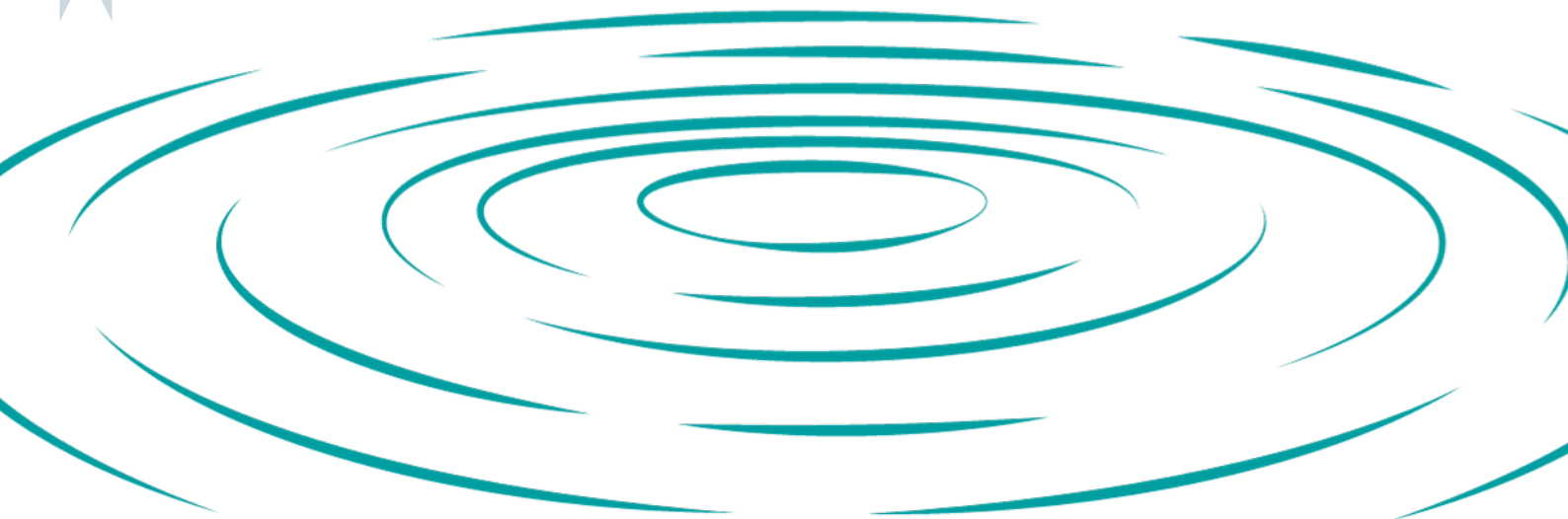
New brain scan study discovers possible biological basis of Visual Snow Syndrome

Last year, Dr Puledda led a study that used a novel approach to show that the patterns of activity in two brain chemical systems - glutamate and serotonin – are different in people with visual snow syndrome compared to those without the condition.

Visual Snow Syndrome (VSS) is characterised by a continuous visual disturbance in which people see static, flickering dots, and flashing lights – this happens when their eyes are both open and closed.

It affects about 2 -3% of the world's population and it can be debilitating, impacting vision, hearing, thinking, sensory processing, and quality of life.

The study was part-funded by the National Institute for Health and Care Research (NIHR) Maudsley Biomedical Research Centre, and supported by the Visual Snow Initiative and the Eye on Vision Foundation.

Researchers used existing scanning data from 24 patients with VSS, 25 migraine patients and 24 healthy people with no VSS or migraine history. The brain scans were conducted at the NIHR King's Clinical Research Facility.

Currently there is no medication that is effective at helping people with VSS and the search for treatment has been hindered by a lack of knowledge around the biology of the condition.

Previous scanning studies in people with VSS have shown alterations in different regions of the brain and how these interact, however, there has been no research looking into the possible molecular changes that could underlie the condition.

Further research into this area could provide insight into potential biological targets for treatment.

Using a new approach that was developed by researchers at the NIHR Maudsley BRC, the study combines information from positron emission tomography (PET) imaging information on the distribution of different chemical receptors in the brain with functional Magnetic Resonance Imaging (fMRI) analysis

of the interaction of activity between different regions of the brain.

Using this Receptor-Enriched Analysis of Functional Connectivity by Targets (REACT) approach, researchers can extract a map of activity of brain chemicals across the different brain areas.

The five brain chemicals examined in this study were noradrenaline, dopamine, serotonin, glutamate and gamma-aminobutyric acid (GABA).

Researchers found that in patients with VSS there were particular differences in the activity of glutamate and serotonin networks in specific areas of the brain.

There was less synchronised activity (or functional connectivity) in the glutamate networks in the anterior cingulate cortex (ACC) in those with VSS compared to healthy controls and those with migraine.

The ACC is a hub for thinking and top-down control over sensory inputs. The different pattern of activity could represent an interruption in the filtering and integration of visual information.

Analysis also showed that VSS patients had reduced functional connectivity in the serotonin networks of the visual cortex, insula, temporal pole and orbitofrontal areas of the brains compared to healthy controls.

This reduced connectivity in serotonin networks was also seen in migraine patients with aura suggesting a biological link between VSS and aura.

The findings suggest that serotonin activity in VSS patients may be influencing the integration of complex sensory information.

The results did not find any differences for the other brain chemicals that were investigated in the study.

Dr Puledda was the first author on the paper publishing these findings, and worked alongside a number of researchers from across the Institute of Psychiatry, Psychology & Neuroscience at King's.

For the full article, published in *Annals of Neurology* in 2023, please see Appendix One at the end of this report.

Dr Francesca Puledda

Senior Clinical Research Fellow
Institute of Psychiatry, Psychology & Neuroscience

Dr Puledda said this on the discovery and its significance:

'Previous research has given us some insight into the brain regions involved in visual snow syndrome but our study is the first to identify the brain chemistry that could underlie the condition and other sensory experiences such as migraine aura.

Until now there have been no effective treatments for VSS and importantly our research has confirmed that VSS is a neurological disorder with a chemical basis that could be used as a target for development of treatments.'

THANK YOU

On behalf of Dr Puledda and King's College London, thank you for your commitment to such critical research.

We are extremely grateful for your generosity and commitment to Dr Puledda's groundbreaking work on Visual Snow Syndrome. We very much look forward to updating you on Dr Puledda's work in our next report.

Your support enables us to impact the lives of those living with Visual Snow Syndrome, by giving them a better understanding of how the syndrome works and affects them. Further research into this area will only serve to progress the chance of finding better ways to treat VSS.

We hope you have enjoyed reading about Dr Francesca Puledda's most recent success.

Thank you.

For more information please contact

Maggy Liu
Senior Philanthropy Manager – International

King's College London & King's Health Partners
Virginia Woolf Building
22 Kingsway
London
WC2B 6LE

Email: Maggy.Liu@kcl.ac.uk

Abnormal Glutamatergic and Serotonergic Connectivity in Visual Snow Syndrome and Migraine with Aura

Francesca Puledda, MD, PhD [1,2] Ottavia Dipasquale, PhD,[2] Benjamin J. M. Gooddy,[3] Nazia Karsan, MRCP, PhD,[1,2] Ray Bose, MD, MD(res),[1,2] Mitul A. Mehta, PhD,[3] Steven C. R. Williams, PhD,[3] and Peter J. Goadsby, MD, PhD[1,2,4]

Objective: Neuropharmacological changes in visual snow syndrome (VSS) are poorly understood. We aimed to use receptor target maps combined with resting functional magnetic resonance imaging (fMRI) data to identify which neurotransmitters might modulate brain circuits involved in VSS.

Methods: We used Receptor-Enriched Analysis of Functional Connectivity by Targets (REACT) to estimate and compare the molecular-enriched functional networks related to 5 neurotransmitter systems of patients with VSS (n = 24), healthy controls (HCs; n = 24), and migraine patients ([MIG], n = 25, 15 of whom had migraine with aura [MwA]). For REACT we used receptor density templates for the transporters of noradrenaline, dopamine, and serotonin, GABA-A and NMDA receptors, as well as $5HT_{1B}$ and $5HT_{2A}$ receptors, and estimated the subject-specific voxel-wise maps of functional connectivity (FC). We then performed voxel-wise comparisons of these maps among HCs, MIG, and VSS.

Results: Patients with VSS had reduced FC in glutamatergic networks localized in the anterior cingulate cortex (ACC) compared to HCs and patients with migraine, and reduced FC in serotoninergic networks localized in the insula, temporal pole, and orbitofrontal cortex compared to controls, similar to patients with migraine with aura. Patients with VSS also showed reduced FC in $5HT_{2A}$-enriched networks, largely localized in occipito-temporo-parietal association cortices. As revealed by subgroup analyses, these changes were independent of, and analogous to, those found in patients with migraine with aura.

Interpretation: Our results show that glutamate and serotonin are involved in brain connectivity alterations in areas of the visual, salience, and limbic systems in VSS. Importantly, altered serotonergic connectivity is independent of migraine in VSS, and simultaneously comparable to that of migraine with aura, highlighting a shared biology between the disorders.

ANN NEUROL 2023;94:873–884

Visual snow refers to a sensory phenomenon characterized by the perception of tiny, constantly moving dots in the entire visual field. When the snow is associated with additional symptoms, such as palinopsia, photophobia, entoptic phenomena, and nyctalopia, one can talk of visual snow syndrome (VSS).[1] VSS presents different degrees of severity[2] and can represent a disabling disorder for many patients,[3] particularly due to its association with migraine,[4] psychiatric disorders,[5] and tinnitus.[6]

Clinical practice and recent studies[7,8] have shown that no medication is particularly effective for VSS, and the search for appropriate treatments has been hindered by the lack of knowledge around the underlying biology of the condition.

A previous magnetic resonance imaging (MRI) study found several changes in the brain functional connectivity (FC) of patients with VSS when compared to healthy controls (HCs). The abnormalities, found both at rest and

during visual stimulus processing, involved a large network of brain areas, particularly the visual pathways, as well as attentional and salience networks.[9] These brain alterations were confirmed with other functional[10,11] and structural[12–14] imaging studies in VSS. A study using [18F]-FDG positron emission tomography (PET) found altered neuronal metabolism in the visual cortex in patients with VSS,[4] and proton magnetic resonance spectroscopy (1H-MRS) showed increased lactate and a trend for increased glutamate in the lingual gyrus.[15]

No study thus far has provided insight into the molecular underpinnings of VSS. Given that VSS seems to involve abnormal sensory processing at the scale of widespread neuronal circuits, this is challenging. However, an altered function of certain neurotransmitters could be hypothesized in the neurobiology of VSS. For example, the close relationship with migraine, as well as evidence of cortical hyperexcitability from neuromodulation studies,[16,17] implicates excitatory and inhibitory imbalance due to either altered glutamatergic and/or GABAergic mechanisms, and possible serotonergic changes.[18]

Here, we aimed to identify biomarkers for the specific brain mechanisms underlying VSS by applying Receptor-Enriched Analysis of Functional Connectivity by Targets (REACT). REACT is a recent multimodal analytical approach comparable to the dual regression (ie, a 2-step multiple linear regression analysis) to estimate subject-specific functional maps from standard templates of the resting state networks.[19] The main difference with the standard dual regression approach is the use of maps of distribution density of molecular targets from PET and single photon emission computed tomography (SPECT) imaging to enrich functional MRI (fMRI) data with molecular information and estimate functional networks related to specific molecular systems of interest.[20] The advantage of REACT is that it allows the use of template-based receptor maps without the need for subject-specific molecular imaging data, whereas also allowing the examination of connectivity changes in light of the molecular mechanisms driving these alterations.

In this work, we revisited fMRI data of both HCs and patients with VSS from our previously published study[9] as a basis for our investigation to look for functional alterations at rest in key neurotransmission-related circuits, including the transporters of noradrenaline (NAT), dopamine (DAT), and serotonin (SERT), the GABA-A and NMDA receptors. We included a third group of patients with migraine, both with and without aura, in order to account for findings due to comorbid migraine diagnosis, as this is a significant comorbidity of VSS that remains to be understood.[21] Finally, we ran a subanalysis focused specifically on serotonin 5HT$_{1B}$ and 5HT$_{2A}$ receptors, as these systems are particularly relevant in migraine[22] and VSS[23] biology.

Methods

Participants
Full details of the original data collection, study population, and study design can be found in the previous publication.[9] In brief, twenty-four patients with VSS (mean age = 28 ± 6 years; men/women = 12/12) and an equal number of gender and age-matched HCs (mean age = 28 ± 5 years; men/women = 10/14) attended a single MRI session. Participants had to be between 20 and 60 years old, with no contraindications to undergo an MRI, no serious previous medical conditions, no history of any recreational drug intake in the past, consumption of no more than 6 cups of coffee per day, no recurrent medication intake with an action on the central nervous system, and no psychological diseases that would require medication or that could affect neural pathways.

The study was granted ethical approval by the London-City and East Research Ethics Committee (Reference number: 16/LO/0964). Informed consent was obtained from all participants.

Twenty-five patients with migraine (21 women and 4 men, 15 with migraine with aura [MwA], 10 with migraine without aura [MWoA], and 19 who were right-handed) from another study in our group[24] were included as a further control cohort.

MRI Acquisition
Scanning was performed on a 3 T General Electric MR750 MRI scanner at the NIHR King's Clinical Research Facility, King's College Hospital, London using a 12-channel radiofrequency (RF) head coil. For HCs and patients with VSS, whole-brain fMRI images were acquired at rest.[15] A multi-echo planar imaging (EPI) sequence was used (TR = 2,500 ms; echo times = 12, 28, 44, and 60 ms; flip angle = 80°; FOV = 240 × 240 mm; matrix = 64 × 64; slice thickness = 3 mm; 32 axial sections collected with sequential [top down] acquisition and 1 mm interslice gap; and in-plane resolution = 3.75 mm). Anatomic scans were also obtained using a high-resolution 3D T1-weighted IR-SPGR sequence (TR = 7.312 ms; TE = 3.016 ms; TI = 400 ms; flip angle = 11; FOV = 270 × 270 mm; matrix = 256 × 256; slice thickness = 1.2 mm; 196 slice partitions, ASSET factor = 1.75; and in-plane resolution = 1 mm).[25]

Image Preprocessing
The rs-fMRI dataset was preprocessed using Analysis of Functional NeuroImages (AFNI)[26] and FMRIB Software Library (FSL).[27] The initial preprocessing steps performed

using afniproc.py included slice timing and volume re-alignment and time-series de-spiking. Mean framewise displacement was also estimated at this stage, using the data from the first echo. TE-dependence analysis was then performed to reduce motion-related artefacts and other non-BOLD sources of noise[25,26] using the tedana workflow.[28] A user-defined mask was applied to the data. An adaptive mask was then generated, in which each voxel's value reflects the number of echoes with "good" data. A 2-stage masking procedure was applied, in which a liberal mask (including voxels with good data in at least the first echo) was used for optimal combination, T2*/S0 estimation, and denoising, whereas a more conservative mask (restricted to voxels with good data in at least the first 3 echoes) was used for the component classification procedure. A monoexponential model was fit to the data at each voxel using log-linear regression in order to estimate T2* and S0 maps. For each voxel, the value from the adaptive mask was used to determine which echoes would be used to estimate T2* and S0. Multi-echo data were then optimally combined using the T2* combination method.[29] Principal component analysis (PCA) based on the PCA component estimation with a Moving Average (stationary Gaussian) process[30] was applied to the optimally combined data for dimensionality reduction. The following metrics were calculated: kappa, rho, countnoise, countsigFT2, countsigFS0, dice_FT2, dice_FS0, signal-noise_t, variance explained, normalized variance explained, and d_table_score. Kappa and Rho were calculated as measures of TE-dependence and TE-independence, respectively. A t test was performed between the distributions of T2*-model F-statistics associated with clusters (ie, signal) and non-cluster voxels (ie, noise) to generate a t-statistic (metric signal-noise_z) and p value (metric signal-noise_p) measuring relative association of the component to signal over noise. The number of significant voxels not from clusters was calculated for each component. Independent component analysis was then used to decompose the dimensionally reduced dataset. The following metrics were calculated: kappa, rho, countnoise, countsigFT2, countsigFS0, dice_FT2, dice_FS0, signal-noise_t, variance explained, normalized variance explained, and d_table_score. Kappa and Rho were calculated as measures of TE-dependence and TE-independence, respectively. A t test was performed between the distributions of T2*-model F-statistics associated with clusters (ie, signal) and non-cluster voxels (ie, noise) to generate a t-statistic (metric signal-noise_z) and p value (metric signal-noise_p) measuring relative association of the component to signal over noise. The number of significant voxels not from clusters was calculated for each component. Next, component selection was performed to identify BOLD

(TE-dependent), non-BOLD (TE-independent), and uncertain (low-variance) components using the Kundu decision tree (version 2.5).[31] This workflow used numpy,[32] scipy,[33] pandas,[34] scikit-learn,[35] nilearn, and nibabel.[36] This workflow also used the Dice similarity index.[37]

White matter (WM) and cerebrospinal fluid (CSF) masks were obtained from the segmentation of the subjects' structural images and eroded in order to minimize the contribution of grey matter partial volume effects. After co-registering them to each individual's fMRI space, they were used to extract the mean WM and CSF signals from each participant's preprocessed dataset. Those signals were then regressed out of the denoised data and a high-pass temporal filter with a cut-off frequency of 0.01 Hz was applied. Data were then spatially smoothed with a with an 8 mm FWHM Gaussian kernel.

Each participant's fMRI dataset was co-registered to its corresponding T1-weighted anatomic scan and warped to standard MNI152 space using the Advanced Normalization Tools.[32] Images were finally resampled at $2 \times 2 \times 2$ mm^3 resolution.

REACT-Based Analysis

For the receptor-enriched fMRI analysis, we ran 2 separate models: the "mixed model," exploring different molecular systems (ie, the dopaminergic, noradrenergic, serotonergic, GABAergic, and glutamatergic systems), and the "serotonergic model," focused on $5HT_{1B}$ and $5HT_{2A}$ receptors (Fig 1). All density maps were derived from in vivo PET images of the transporters of dopamine,[38] noradrenaline,[39] and serotonin (derived from an internal PET database of [^{11}C]DASB PET images of 16 healthy controls), as well as the GABA-A,[40] and NMDA (derived from an internal database of [^{18}F]GE-179 PET images of 9 HCs). $5HT_{1B}$ and $5HT_{2A}$ receptors were used to enrich the functional data with information on the spatial density distribution for each target. Of note, both models included the density map of SERT. However, whereas in the mixed model the distribution of SERT was used to capture the full architecture of serotonin and explore the brain's functional mechanisms underlying VSS, in the serotonergic model it was included only to control for its effects in the primary responses of interest, that is, those related to $5HT_{1B}$ and $5HT_{2A}$ receptors.

Running REACT comprises of a 2-step multiple linear regression analysis within the REACT toolbox (https://github.com/ottaviadipasquale/react-fmri).[41] The 4D whole-brain fMRI maps and PET maps were demeaned, and the PET maps used as spatial regressors to estimate the dominant BOLD fluctuations related to each
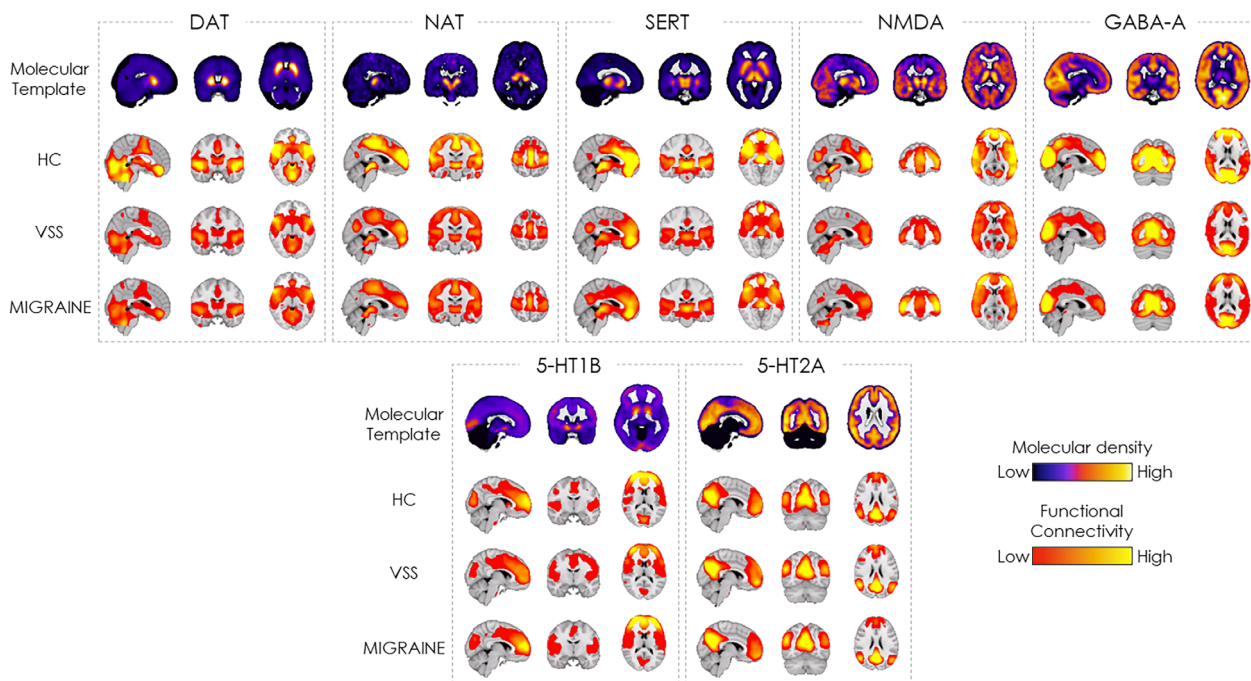
FIGURE 1: PET maps used within REACT for the molecular targets of DAT, NAT, SERT, NMDA, and GABA-A (upper panel), $5HT_{1B}$ and $5HT_{2A}$ (lower panel) with relative functional connectivity maps averaged across each group. DAT = dopamine; HC = healthy control; NAT = noradrenaline; PET = positron emission tomography; REACT = Receptor-Enriched Analysis of Functional Connectivity by Targets; SERT = serotonin; VSS = visual snow syndrome.

of the molecular targets. Of note, a mask, generated by binarizing the PET maps, was used to restrict analysis to only the areas where information on transporter and receptor density was available. This first step of this analysis generated subject-specific temporal dynamics for each of the molecular targets, which were then used as temporal regressors in the second multiple linear regression to estimate molecular-enriched functional connectivity maps. At this stage, the input fMRI data and design matrix were demeaned, with additional normalization of the latter to unit standard deviation, and the analysis was conducted on the whole grey matter volume. This final step of REACT generated, for each combination of participant (VSS, HCs, and MIG) FC maps enriched by the molecular systems included in each model (mixed and serotonergic).

Statistical Analysis

For each molecular-enriched functional network of interest resulting from the 2 models (ie, DAT, NAT, SERT, NMDA, and GABA-A for the mixed model, and $5HT_{1B}$ and $5HT_{2A}$ for the serotonergic model), we first compared the subject-specific spatial maps across groups (HC, VSS, and MIG) using permutation-based 1-way analysis of covariance (ANCOVAs), controlling for mean framewise displacement. Additionally, to test if the changes found in the main analysis were unique to VSS, we ran subgroup

1-way ANCOVAs comparing HCs, pure VSS (ie, patients with VSS with no migraine), and MwoA; and HCs, pure VSS, and MwA. All voxel-wise statistical analyses were performed with Randomise,[42] using 5,000 permutations per test and contrast. Multiple comparison errors were controlled for by using the threshold-free cluster enhancement option[43] in FSL.

For each significant result, we extracted the mean FC values within the significant clusters and ran Tukey post hoc tests in SPSS to evaluate which groups differed from each other, controlling for mean framewise displacement.

Results

One patient with VSS and three HCs were excluded from final analyses due to excessive head movement (mean framewise displacement > 0.2 mm). No patients with migraine were excluded. This left n = 23 patients in the VSS group, of whom n = 9 had no migraine ("pure VSS" group), n = 21 patients in the HC group and 25 patients in the migraine group (MIG), of whom 15 had aura (MwA group).

The molecular-enriched FC maps related to DAT, NAT, SERT, NMDA, GABA-A, $5HT_{1B}$, and $5HT_{2A}$, averaged across each group (HCs, patients with VSS, and patients with migraine), are reported in Figure 1.

Mixed Model

The 1-way ANCOVAs highlighted statistically significant differences between the HC, VSS, and the MIG groups in the functional networks enriched with SERT and NMDA (Fig 2A) and localized in the right insula, temporal pole, and orbitofrontal cortex ($F_{peak} = 14.5$, $p = 0.009$, number of voxels = 761, $x_{peak} = 40$, $y_{peak} = 12$, $z_{peak} = -22$) and in the anterior cingulate cortex (ACC)/middle cingulate cortex (MCC; $F_{peak} = 14.2$, $p = 0.042$, number of voxels = 26, $x_{peak} = 60$, $y_{peak} = 0$, $z_{peak} = 38$), respectively. Tukey post hoc tests revealed lower FC in the SERT-enriched network in patients (both VSS and migraine) as compared to HCs (VSS < HC, $t = 5.160$,

$p < 0.001$; MIG < HC, $t = 4.417$, $p < 0.001$), and in the NMDA-enriched network in VSS with respect to HCs and patients with migraine (VSS < HC, $t = 5.252$, $p < 0.001$; VSS < MIG, $t = 4.598$, $p < 0.001$). No group differences were found for DAT-, NAT-, and GABA-A-enriched functional networks.

When comparing HCs and the 2 subgroups "pure VSS" and MwoA in the same model, we found significant differences in the NMDA-enriched functional network localized in right frontal pole, inferior and middle frontal gyri (Fig 2B; $F_{peak} = 16.9$, $p = 0.010$, number of voxels = 937, $x_{peak} = 38$, $y_{peak} = 36$, $z_{peak} = 6$). Post hoc analyses revealed higher FC in MwoA as compared to HC
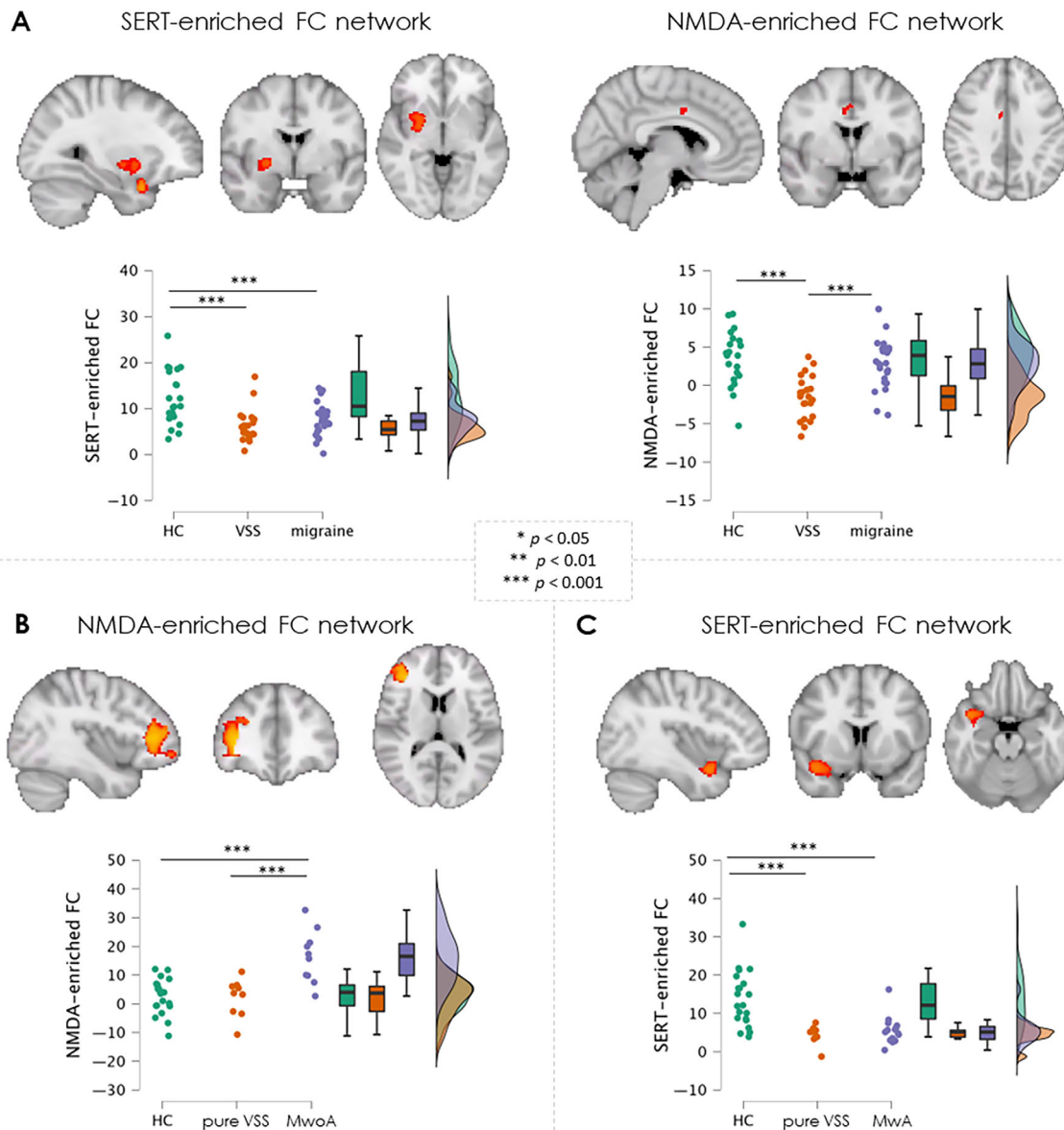

FIGURE 2: Mixed model analysis. (A) Full group analysis showing significant changes in SERT (left) and NMDA (right) enriched networks in patients with VSS with respect to HCs and patients with MIG groups. (B) Subgroup analysis comparing HC versus pure VSS versus MwoA. (C) Subgroup analysis comparing HCs versus patients with pure VSS versus patients with MwA. HCs = healthy controls; MIG = migraine; MwA = migraine with aura; MwoA = migraine without aura; SERT = serotonin transporter; VSS = visual snow syndrome.

(t-stat = 5.37, $p < 0.001$) and pure VSS ($t = 4.753$, $p < 0.001$). No significant differences were found in the other systems.

When comparing HCs and the 2 subgroups "pure VSS" and MwA, we found significant differences in the SERT-enriched functional network localized in the right temporal pole, insula, orbitofrontal cortex, and planum polare (Fig 2C; $F_{peak} = 15.3$, $p = 0.023$, number of voxels = 256, $x_{peak} = 40$, $y_{peak} = 8$, $z_{peak} = -20$). Post hoc analyses revealed lower FC in both patients with pure VSS and with MwoA as compared to HCs (pure VSS < HC, $t = 4.164$, $p < 0.001$; MwA < HC, $t = 4.576$, $p < 0.001$). No significant differences were found in the other systems.

Serotonin Model

The one-way ANCOVAs highlighted statistically significant differences among the HCs, VSS, and MIG groups in 5 clusters of the $5HT_{2A}$-enriched functional network (Fig 3 and Table , upper panel). These clusters were localized in different cortical regions, including the right planum temporale, central opercular cortex, Heschl's gyrus, planum polare, superior temporal gyrus, postcentral gyrus, supramarginal gyrus, parietal operculum cortex and insula (cluster 1), the left postcentral gyrus, opercular cortex, superior temporal gyrus, planum temporale, planum polare, and Heschl's gyrus (cluster 2), the right superior and inferior division of the lateral occipital cortex and the right middle and inferior temporal gyrus (cluster 3), the left inferior division of the lateral occipital cortex (cluster 4), and the right temporal occipital fusiform cortex and occipital fusiform gyrus (cluster 5). Tukey post hoc tests

revealed lower FC in patients (both the VSS and MIG groups) as compared to HCs in all clusters (see "Significant contrasts" column in Table). No group differences were found in the $5HT_{1B}$-enriched functional network.

The subgroup ANCOVAs comparing HCs, patients with pure VSS, and patients with MwoA showed significant differences in 3 clusters of the $5HT_{2A}$-enriched network (see Table , middle panel). The first 2 clusters vastly overlap with clusters 3 and 4 of the full group analysis, whereas the third is located in the right inferior division of the lateral occipital cortex and the right occipital fusiform gyrus. The post hoc tests revealed significantly lower FC in both patient subgroups compared to HCs in cluster 1, and lower FC in pure VSS compared to HC and MwoA in clusters 2 and 3. No group differences were found in the $5HT_{1B}$-enriched functional network.

The subgroup ANCOVAs comparing HCs, patients with pure VSS, and patients with migraine with aura showed significant differences in 9 clusters of the $5HT_{2A}$-enriched network (Fig 4 and Table , lower panel). The post hoc tests revealed lower FC in patients (both VSS and MwA) as compared to HCs in all clusters excluding the smallest one (see "Significant effect" column in Table). No group differences were found in the $5HT_{1B}$-enriched functional network.

Discussion

The data presented here show that patients with VSS demonstrate significant differences in functional brain networks related to SERT and NMDA molecular systems,
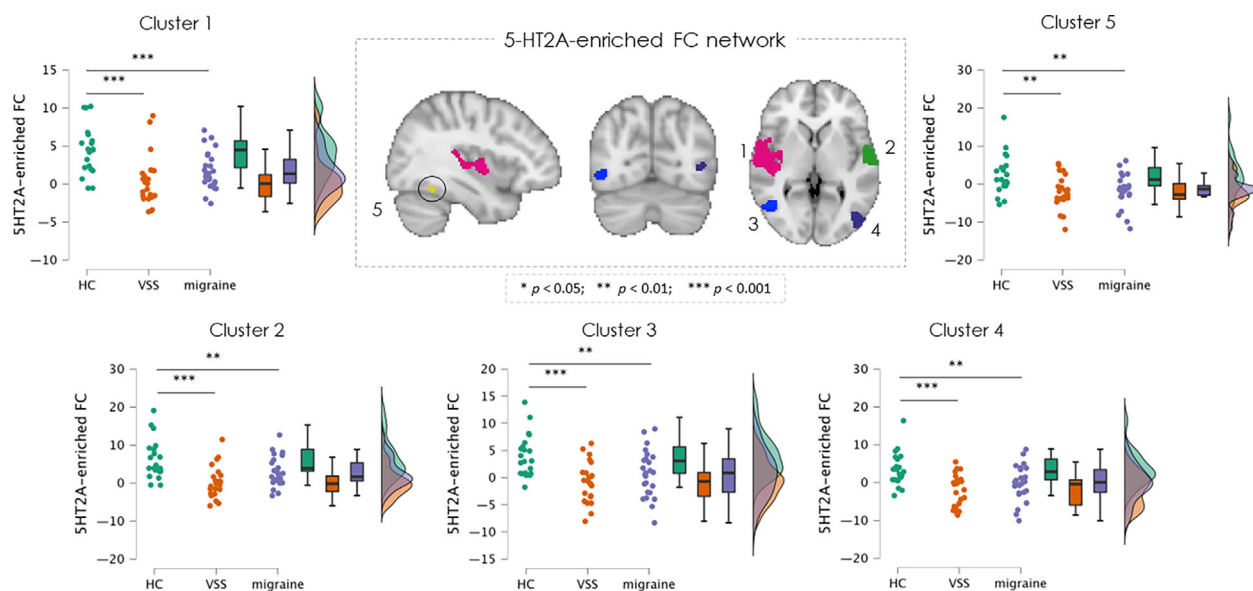

FIGURE 3: Clusters of significantly reduced serotonergic-enriched functional connectivity in all patients with VSS (n = 23) and patients with MIG (n = 25) with respect to HCs (n = 21). For all values and statistics refer to Table . FC = functional connectivity; HCs = healthy controls; MIG = migraine; VSS = visual snow syndrome.

TABLE. Clusters Showing Significant Molecular-Enriched FC Differences for the 5HT$_{2A}$ Target of the Serotonin Model, Comparing the Full Groups (Patients With VSS, HC, and MIG; upper panel); and Two Subgroup Analyses: Pure VSS, HC, and MwoA (Middle Panel); Pure VSS, HC, and MwA (Lower Panel)

Group comparison	F_{peak}	$P_{(FWE)}$	k	x	y	z	Brain regions	Significant contrasts	t	p
					F-test			Post hoc tests		
VSS versus HC versus MIG	16.7	0.004	2,119	46	−28	6	R PT, central operculum, HG, PP, STG, PoG, SMG, parietal operculum, and insula	HC > VSS	5.803	< 0.001
								HC > MIG	4.461	< 0.001
	13.1	0.015	657	−58	−6	2	L PoG, opercular cortex, STG, PT, PP, and HG	HC > VSS	5.117	< 0.001
								HC > MIG	3.425	0.003
	12.4	0.025	303	46	−62	2	R superior and inferior LO; MTG, and ITG	HC > VSS	4.582	< 0.001
								HC > MIG	3.59	0.002
	11.5	0.031	232	−50	−80	0	L inferior division of LO	HC > VSS	4.428	< 0.001
								HC > MIG	3.34	0.004
	8.34	0.047	35	34	−50	−16	R FG	HC > VSS	3.551	0.002
								HC > MIG	3.567	0.002
Pure VSS versus HC versus MwoA	13.7	0.036	175	44	−62	2	R superior and inferior LO, MTG, and ITG	HC > pure VSS	4.977	< 0.001
								HC > MwoA	2.755	0.024
	18.5	0.028	136	−46	−80	−2	L inferior LO	HC > pure VSS	5.908	< 0.001
								MwoA > pure VSS	3.121	0.01
	11.3	0.048	22	46	−66	−18	R inferior LO and FG	HC > pure VSS	4.715	< 0.001
								MwoA > pure VSS	2.443	0.05
Pure VSS versus HC versus MwA	15.4	0.014	1,044	62	−18	20	R central operculum; PoG, PT, PP, HG, SMG, STG, and parietal operculum	HC > pure VSS	5.004	< 0.001
								HC > MwA	4.654	< 0.001
	18.8	0.01	964	46	−62	2	R LO; MTG; and FG	HC > pure VSS	5.012	< 0.001
								HC > MwA	3.395	0.004
	17.1	0.012	745	−54	−10	0	L central operculum, Insula, PP, STG, PT, and HG	HC > pure VSS	4.44	< 0.001
								HC > MwA	4.791	<0.001
	15.9	0.03	169	−48	−82	0	L LO	HC > pure VSS	5.248	< 0.001
								HC > MwA	3.19	0.008
	20.2	0.019	155	28	−54	50	R superior parietal lobule; LO; and AG	HC > pure VSS	5.468	< 0.001
								HC > MwA	3.72	0.002
	10.4	0.039	96	38	−6	2	R insula	HC > pure VSS	3.911	< 0.001
								HC > MwA	3.7	0.002
	11.9	0.036	89	−56	−20	20	L central operculum PoG, parietal operculum, and SMG	HC > pure VSS	3.975	< 0.001
								HC > MwA	3.734	0.002
	8.9	0.047	18	44	−30	8	R PT, HG, and STG	HC > pure VSS	3.732	0.002
								HC > MwA	3.17	0.008
	8.2	0.049	10	32	−72	−16	R FG, LO, and LG	HC > pure VSS	3.967	< 0.001
								HC > MwA	1.975	0.131

Abbreviations: AG = angular gyrus; FG = fusiform gyrus; HC = healthy control; HG = Heschl's gyrus; ITG = inferior temporal gyrus; k = cluster size; L = left; LG = lingual gyrus; LO = lateral occipital cortex; MIG = migraine; MTG = middle temporal gyrus; MwA = migraine with aura; MwoA = migraine without aura; PP = planum polare; PoG = postcentral gyrus; PT = planum temporale; R = right; SMG = supramarginal gyrus; STG = superior temporal gyrus; VSS = visual snow syndrome.
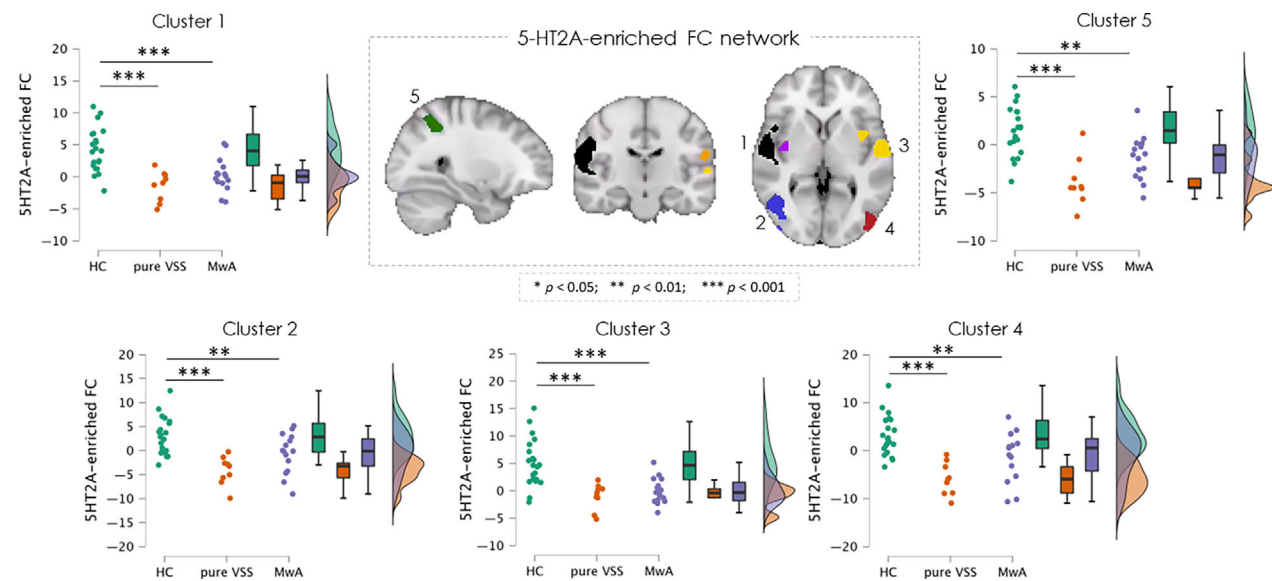
FIGURE 4: Clusters of significantly decreased 5HT$_{2A}$-enriched functional connectivity in patients with pure VSS (n = 9) and MwA (n = 15) with respect to HCs (n = 21). For all values and statistics refer to Table ; only cluster with > 100 voxels are shown in the image. FC = functional connectivity; HCs = healthy controls; MwA = migraine with aura; VSS = visual snow syndrome.

and not GABA-A and NAT, with respect to HCs. These changes, involving crucial areas of the sensory and limbic systems, not only confirm functional connectivity alterations of VSS found in previous studies, but also allow us to view those findings in light of molecular mechanisms that could be specific to the syndrome. Importantly, all regions of significantly differing connectivity found in patients with VSS were indeed opposite to the direction of coupling shown in the averaged neurotransmitter maps (see Fig 1). This confirms that the areas of gain or decrease of connectivity diverge significantly from the normal function of these brain networks, and might thus represent a robust biomarker of VSS. This is corroborated by the comparison with the migraine patient group and by the subgroup analyses conducted in patients with VSS and no migraine, which suggested that the changes were largely independent of migraine co-occurrence in VSS. In fact, consistent with previous reports in the literature,[2,4] 60% of our VSS population had concomitant migraine. In order to make inferences regarding the disorder's specific pathophysiology, it is therefore of crucial importance to distinguish the neural changes of interictal migraine from those inherent to VSS.

Among our findings from the mixed model, accounting for the influence of different neurotransmitter systems in the functional connectivity changes in VSS, we were able to establish that glutamatergic-enriched connectivity is uniquely reduced in VSS in the dorsal ACC/MCC (see Fig 2A). This region has connections to both the limbic system and executive areas of the frontal and parietal cortices,[44] making it an important hub for cognition and top-down sensory control.[45] The anterior/mid-cingulate cortex is directly involved in attentional and salience processes[46,47] as well as executive awareness functions.[48,49]

Glutamate alterations have been detected in the visual cortex of patients with VSS by means of MRS.[15] As the major excitatory neurotransmitter in the brain, glutamate is considered a key factor in states of altered excitability and hyper-responsivity, such as migraine.[50] A reduced glutamate-mediated connectivity in this region in VSS might thus signify a dysregulation of normal attentional functions and integration of sensory processing[51] that cannot be explained by a simple cortical hyper-excitability, rather by a the wider spectrum of cortical dys-excitability that is common to migraine with aura as well.[52,53] Further, the fact that NMDA-related activity was associated with reduced connectivity in the mid-cingulate cortex suggests downregulation of multi-sensory control mechanisms in these brain regions,[54] and could even represent a potential pharmacological target for VSS in the future.

Patients with VSS also showed changes in connectivity associated with areas of serotoninergic transporter expression, represented by decreased FC in the insula, temporal pole, and orbitofrontal cortex, similar to that of patients with migraine. When analyzing this in more detail by looking at our population subgroups (see Fig 2C), the change was confirmed in patients with "pure VSS," and was equally present in patients with migraine with aura, but not in those without aura. The anterior insula is a central station within the salience network,[55] which can be understood as the areas adapting behavior

based on the internal predictions created by the brain and on how much these deviate from the external environment.[56,57] The posterior regions of the insula are associated with somatotopic organization and nociceptive detection, with input directed to the more anterior areas.[58] The involvement of the orbitofrontal cortex and temporal pole might further be linked to the concomitant presence of tinnitus in patients with VSS, as these regions are directly implicated in different levels of auditory stimulus processing.[59,60] Overall, these findings suggest that serotonin might be influencing the dysregulated integration of complex sensory stimuli typical of VSS.

The serotonin model allowed us to investigate these changes with more detail. Here, we found that FC was reduced in VSS in a 5HT$_{2A}$-dominated network localized bilaterally in the insula, primary and secondary auditory cortices, and in areas V3/V3A and V5 of the associative visual cortex. Area V5 represents the main region of the visual system to detect motion stimuli[61] and has previously been implicated in VSS neurobiology, with findings of increased grey matter volume in this region,[12] coherent with the perception of moving dots central to the condition. Area V3/V3A, on the other hand, has never been investigated in VSS; it has, however, a long-standing association with typical migraine aura, mostly thanks to a seminal paper showing early activation of this region at the onset of visual aura symptoms.[62] Area V3A has a retinotopic representation of the opposite hemifield and is associated with motion processing,[63] which could certainly explain its relevance in VSS.[64]

Importantly, by analyzing patients with VSS with no migraine, as well as patients with migraine with or without aura, we found that these areas showed overlapping and independent FC changes in "pure VSS" and migraine with aura. This finding could thus provide a missing link to explain the complex pathophysiology among VSS, migraine, and typical migraine with aura. In fact, whereas the association between migraine without aura and VSS is characterized by co-occurrence of the 2 disorders, reflected by a worsened phenotype of VSS when migraine is also present,[2] typical aura is more common in VSS without making the disorder more severe. This suggests that the link between typical aura and VSS is a purely biological one, rather than a bi-directional worsening of one condition in the presence of the other.[4]

Aberrant serotoninergic metabolism has also been implicated in visual perceptual syndromes,[65] particularly hallucinogen persisting perception disorder (HPPD).[66,67] HPPD typically arises following consumption of lysergic acid diethylamide, a potent partial 5HT$_{2A}$ receptor agonist.[68–70] It has strong pathophysiological links to VSS,[2] often presenting with overlapping symptomatology.[71] The 5-HT$_{2A}$ receptor is abundantly expressed in layers III and V of the brain's visual cortex, particularly in inhibitory interneurons within V1 and V2[72,73] and an imbalance between cortical excitation and inhibition mechanisms has long been suspected in HPPD.[74] It is thus not surprising that the activity of serotonin and the 5-HT$_{2A}$ receptor may be associated with a disruption of visual and salience networks in VSS, particularly given the high density of serotoninergic projections from the thalamus and LGN to the visual cortex.[75] Interestingly, a recent case reported VSS symptoms arising after exposure to citalopram, a selective serotonin reuptake inhibitor.[23] Further, lamotrigine, which has an inhibitory function on 5HT$_{2A}$ receptors and is widely used in patients with typical migraine aura and HPPD,[76] has also shown anecdotal efficacy in VSS.[7] However, a larger case series has shown that both citalopram and lamotrigine are mostly inert in patients with VSS,[8] thus suggesting that serotoninergic transmission has a more complex role in the biology of this condition.

An interpretation of our current findings is that serotonin might be modulating the altered connectivity within areas of the visual motion network in VSS, via dysfunction in the salience network, and could thus be causing wrongful allocation of attention to the noise-like percept of snow and increased neural gain within the visual system.[77] Our findings further provide evidence for a serotonin-5HT$_{2A}$ involvement in the pathophysiological association among VSS, migraine with aura, and HPPD.

Limitations

The main limitations of our study relate to the relatively small sample size, which could certainly have influenced our final results. However, the functional connectivity analysis has shown to be powered adequately, as it demonstrated effects related to visual snow in our previous study.[9] Second, although REACT improves the interpretability of resting-state analyses, it does not measure neurotransmitter function directly and relies on molecular templates of healthy subjects estimated independently. Finally, although the imaging parameters and study location were identical, the migraine cohort was added subsequently for analysis purposes and thus did not form part of the original study.

Conclusions

In conclusion, our results show that glutamatergic and serotoninergic circuits are directly involved in the dysfunctional activity of visual and salience networks in VSS, and could represent potential drug targets for the condition in the future. The brain regions most involved in these changes were the insula and ACC, supplementary visual areas V3/V3A and V5, and the auditory cortices. Our

findings also suggest that altered serotonergic connectivity might represent the common link among VSS, HPPD, and migraine with aura.

Author Contributions

F.P., O.D., S.C.R.W., and P.J.G. were responsible for the conception and design of the study. F.P., O.D., B.J.M.G., N.K., R.B., and S.C.R.W. were responsible for the acquisition and analysis of data. F.P., O.D., B.J.M.G., M.A.M., S.C.R.W., and P.J.G. were responsible for the drafting of a significant portion of the manuscript.

Potential Conflicts of Interest

The authors declare no conflict of interest relevant for this manuscript.

References

1. Schankin CJ, Maniyar FH, Digre KB, Goadsby PJ. 'Visual snow'-a disorder distinct from persistent migraine aura. Brain 2014;137:1419–1428.

2. Puledda F, Schankin C, Goadsby PJ. Visual snow syndrome. A clinical and phenotypical description of 1,100 cases. Neurology 2020;94:e564–e574.

3. Schankin CJ, Puledda F, Goadsby PJ. Visual snow syndrome: is it normal or a disorder-and what to do with patients? Eur J Neurol 2020;27:2393–2395.

4. Schankin CJ, Maniyar FH, Sprenger T, et al. The relation between migraine, typical migraine aura and "visual snow". Headache 2014;54:957–966.

5. Solly EJ, Clough M, Foletta P, et al. The psychiatric symptomology of visual snow syndrome. Front Neurol 2021;12:703006.

6. Lauschke JL, Plant GT, Fraser CL. Visual snow: a thalamocortical dysrhythmia of the visual pathway? J Clin Neurosci 2016;28:123–127.

7. van Dongen RM, Waaijer LC, Onderwater GLJ, et al. Treatment effects and comorbid diseases in 58 patients with visual snow. Neurology 2019;93:e398–e403.

8. Puledda F, Vandenbussche N, Moreno-Ajona D, et al. Evaluation of treatment response and symptom progression in 400 patients with visual snow syndrome. Br J Ophthalmol 2022;106:1318–1324.

9. Puledda F, O'Daly O, Schankin C, et al. Disrupted connectivity within visual, attentional and salience networks in the visual snow syndrome. Hum Brain Mapp 2021;42:2032–2044.

10. Puledda F, Schankin CJ, O'Daly O, et al. Localised increase in regional cerebral perfusion in patients with visual snow syndrome: a pseudo-continuous arterial spin labelling study. J Neurol Neurosurg Psychiatry 2021;92:918–926.

11. Aldusary N, Traber GL, Freund P, et al. Abnormal connectivity and brain structure in patients with visual snow. Front Hum Neurosci 2020;14:582031.

12. Puledda F, Bruchhage M, O'Daly O, et al. Occipital cortex and cerebellum gray matter changes in visual snow syndrome. Neurology 2020;95:e1792–e1799.

13. Schankin CJ, Maniyar FH, Chou DE, et al. Structural and functional footprint of visual snow syndrome. Brain 2020;143:1106–1113.

14. Strik M, Clough M, Solly EJ, et al. Microstructure in patients with visual snow syndrome: an ultra-high field morphological and quantitative MRI study. Brain Commun 2022;4:fcac164.

15. Puledda F, Ffytche D, Lythgoe DJ, et al. Insular and occipital changes in visual snow syndrome: a BOLD fMRI and MRS study. Ann Clin Transl Neurol 2020;7:296–306.

16. Yildiz FG, Turkyilmaz U, Unal-Cevik I. The clinical characteristics and neurophysiological assessments of the occipital cortex in visual snow syndrome with or without migraine. Headache 2019;59:484–494.

17. Eren O, Rauschel V, Ruscheweyh R, et al. Evidence of dysfunction in the visual association cortex in visual snow syndrome. Ann Neurol 2018;84:946–949.

18. Ferrari MD, Odink J, Tapparelli C, et al. Serotonin metabolism in migraine. Neurology 1989;39:1239–1242.

19. Martins D, Veronese M, Turkheimer FE, et al. A candidate neuroimaging biomarker for detection of neurotransmission-related functional alterations and prediction of pharmacological analgesic response in chronic pain. Brain Commun 2021;4:fcab302.

20. Dipasquale O, Selvaggi P, Veronese M, et al. Receptor-enriched analysis of functional connectivity by targets (REACT): a novel, multimodal analytical approach informed by PET to study the pharmacodynamic response of the brain under MDMA. Neuroimage 2019;195:252–260.

21. Silva EM, Puledda F. Visual snow syndrome and migraine: a review. Eye 2023.

22. Goadsby PJ, Lipton RB, Ferrari MD. Migraine—current understanding and treatment. N Engl J Med 2002;346:257–270.

23. Eren OE, Schöberl F, Schankin CJ, Straube A. Visual snow syndrome after start of citalopram—novel insights into underlying pathophysiology. Eur J Clin Pharmacol 2021;77:271–272.

24. Karsan N, Bose PR, O'Daly O, et al. Alterations in functional connectivity during different phases of the triggered migraine attack. Headache 2020;60:1244–1258.

25. Jack CR Jr, Bernstein MA, Borowski BJ, et al. Update on the magnetic resonance imaging core of the Alzheimer's disease neuroimaging initiative. Alzheimers Dement 2010;6:212–220.

26. Cox RW. AFNI: software for analysis and visualization of functional magnetic resonance neuroimages. Comput Biomed Res 1996;29:162–173.

27. Jenkinson M, Beckmann CF, Behrens TEJ, et al. FSL. Neuroimage 2012;62:782–790.

28. DuPre EM, Salo T, Ahmed Z, et al. TE-dependent analysis of multi-echo fMRI with tedana. J Open Source Software 2021;6:3669.

29. Posse S, Wiese S, Gembris D, et al. Enhancement of BOLD-contrast sensitivity by single-shot multi-echo functional MR imaging. Magn Reson Med 1999;42:87–97.

30. Li YO, Adali T, Calhoun VD. Estimating the number of independent components for functional magnetic resonance imaging data. Hum Brain Mapp 2007;28:1251–1266.

31. Kundu P, Brenowitz ND, Voon V, et al. Integrated strategy for improving functional connectivity mapping using multiecho fMRI. Proc Natl Acad Sci U S A 2013;110:16187–16192.

32. van der Walt S, Colbert SC, Varoquaux G. The NumPy Array: a structure for efficient numerical computation. Comput Sci Eng 2011;13:22–30.

33. Virtanen P, Gommers R, Oliphant TE, et al. SciPy 1.0: fundamental algorithms for scientific computing in python. Nat Methods 2020;17:261–272.

34. McKinney W. Data structures for statistical computing in python. 9th Python in Science Conference, 2010:51-56.

35. Pedregosa F, Varoquaux G, Gramfort A, et al. Scikit-learn: machine learning in python. J Mach Learn Res 2011;12:2825–2830.

36. Brett M, Markiewicz CJ, Hanke M, et al. nipy/nibabel: 5.1.0 (5.1.0). Zenodo, https://zenodo.org/record/4295521.

37. Dice LR. Measures of the amount of ecologic association between species. Ecology 1945;26:297–302.

38. García-Gómez FJ, García-Solís D, Luis-Simón FJ, et al. Elaboration of the SPM template for the standardization of SPECT images with 123I-Ioflupane. Rev Esp Med Nucl Imagen Mol 2013;32:350–356.

39. Hesse S, Becker G-A, Rullmann M, et al. Central noradrenaline transporter availability in highly obese, non-depressed individuals. Eur J Nucl Med Mol Imaging 2017;44:1056–1064.

40. Nørgaard M, Beliveau V, Ganz M, et al. A high-resolution in vivo atlas of the human brain's benzodiazepine binding site of GABA(a) receptors. Neuroimage 2021;232:117878.

41. Dipasquale O, Cohen A, Martins D, et al. Molecular-enriched functional connectivity in the human brain using multiband multi-echo simultaneous ASL/BOLD fMRI. Sci Rep 2023;13:11751.

42. Winkler AM, Ridgway GR, Webster MA, et al. Permutation inference for the general linear model. Neuroimage 2014;92:381–397.

43. Smith SM, Nichols TE. Threshold-free cluster enhancement: addressing problems of smoothing, threshold dependence and localisation in cluster inference. Neuroimage 2009;44:83–98.

44. Beckmann M, Johansen-Berg H, Rushworth MF. Connectivity-based parcellation of human cingulate cortex and its relation to functional specialization. J Neurosci 2009;29:1175–1190.

45. Bush G, Luu P, Posner MI. Cognitive and emotional influences in anterior cingulate cortex. Trends Cogn Sci 2000;4:215–222.

46. Pardo JV, Pardo PJ, Janer KW, Raichle ME. The anterior cingulate cortex mediates processing selection in the Stroop attentional conflict paradigm. Proc Natl Acad Sci U S A 1990;87:256–259.

47. Seeley WW, Menon V, Schatzberg AF, et al. Dissociable intrinsic connectivity networks for salience processing and executive control. J Neurosci 2007;27:2349–2356.

48. Allman JM, Hakeem A, Erwin JM, et al. The anterior cingulate cortex. Ann N Y Acad Sci 2001;935:107–117.

49. Vogt BA, Derbyshire S, Jones AK. Pain processing in four regions of human cingulate cortex localized with co-registered PET and MR imaging. Eur J Neurosci 1996;8:1461–1473.

50. Coppola G, Pierelli F, Schoenen J. Is the cerebral cortex hyper-excitable or hyperresponsive in migraine? Cephalalgia 2007;27:1427–1439.

51. Goadsby PJ, Holland PR, Martins-Oliveira M, et al. Pathophysiology of migraine- a disorder of sensory processing. Physiol Rev 2017;97:553–622.

52. Chen WT, Lin YY, Fuh JL, et al. Sustained visual cortex hyper-excitability in migraine with persistent visual aura. Brain 2011;134:2387–2395.

53. Stankewitz A, May A. The phenomenon of changes in cortical excitability in migraine is not migraine-specific–a unifying thesis. Pain 2009;145:14–17.

54. Vogt BA. Midcingulate cortex: structure, connections, homologies, functions and diseases. J Chem Neuroanat 2016;74:28–46.

55. Menon V, Uddin LQ. Saliency, switching, attention and control: a network model of insula function. Brain Struct Funct 2010;214:655–667.

56. Shelley BP, Trimble MR. The insular lobe of Reil–its Anatamico-functional, behavioural and neuropsychiatric attributes in humans–a review. World J Biol Psychiatry 2004;5:176–200.

57. Billeke P, Ossandon T, Perrone-Bertolotti M, et al. Human anterior insula encodes performance feedback and relays prediction error to the medial prefrontal cortex. Cereb Cortex 2020;30:4011–4025.

58. Frot M, Faillenot I, Mauguière F. Processing of nociceptive input from posterior to anterior insula in humans. Hum Brain Mapp 2014;35:5486–5499.

59. Leaver AM, Renier L, Chevillet MA, et al. Dysregulation of limbic and auditory networks in tinnitus. Neuron 2011;69:33–43.

60. Kringelbach ML. The human orbitofrontal cortex: linking reward to hedonic experience. Nat Rev Neurosci 2005;6:691–702.

61. Watson JD, Myers R, Frackowiak RS, et al. Area V5 of the human brain: evidence from a combined study using positron emission tomography and magnetic resonance imaging. Cereb Cortex 1993;3:79–94.

62. Hadjikhani N, Sanchez Del Rio M, Wu O, et al. Mechanisms of migraine aura revealed by functional MRI in human visual cortex. Proc Natl Acad Sci U S A 2001;98:4687–4692.

63. Tootell RB, Mendola JD, Hadjikhani NK, et al. Functional analysis of V3A and related areas in human visual cortex. J Neurosci 1997;17:7060–7078.

64. Puledda F, Ffytche DH, O'Daly O, Goadsby PJ. Imaging the visual network in the migraine Spectrum. Front Neurol 2019;10:1325.

65. Ffytche DH. Visual hallucinatory syndromes: past, present, and future. Dialogues Clin Neurosci 2007;9:173–189.

66. Kilpatrick ZP, Bard EG. Hallucinogen persisting perception disorder in neuronal networks with adaptation. J Comput Neurosci 2012;32:25–53.

67. Abraham HD. Visual phenomenology of the LSD flashback. Arch Gen Psychiatry 1983;40:884–889.

68. Abraham HD, Aldridge AM, Gogia P. The psychopharmacology of hallucinogens. Neuropsychopharmacology 1996;14:285–298.

69. Aghajanian GK, Marek GJ. Serotonin and hallucinogens. Neuropsychopharmacology 1999;21:16s–23s.

70. Lawn T, Dipasquale O, Vamvakas A, et al. Differential contributions of serotonergic and dopaminergic functional connectivity to the phenomenology of LSD. Psychopharmacology (Berl) 2022;239:1797–1808.

71. van Dongen RM, Alderliefste GJ, Onderwater GLJ, et al. Migraine prevalence in visual snow with prior illicit drug use (hallucinogen persisting perception disorder) versus without. Eur J Neurol 2021;28:2631–2638.

72. Zilles K, Palomero-Gallagher N, Grefkes C, et al. Architectonics of the human cerebral cortex and transmitter receptor fingerprints: reconciling functional neuroanatomy and neurochemistry. Eur Neuropsychopharmacol 2002;12:587–599.

73. Litjens RP, Brunt TM, Alderliefste GJ, Westerink RH. Hallucinogen persisting perception disorder and the serotonergic system: a

comprehensive review including new MDMA-related clinical cases. Eur Neuropsychopharmacol 2014;24:1309–1323.

74. Abraham HD, Aldridge AM. Adverse consequences of lysergic acid diethylamide. Addiction 1993;88:1327–1334.

75. Burnet PW, Eastwood SL, Lacey K, Harrison PJ. The distribution of 5-HT1A and 5-HT2A receptor mRNA in human brain. Brain Res 1995;676:157–168.

76. Martinotti G, Santacroce R, Pettorruso M, et al. Hallucinogen persisting perception disorder: etiology, clinical features, and therapeutic perspectives. Brain Sci 2018;8:47.

77. Brooks CJ, Chan YM, Fielding J, et al. Visual contrast perception in visual snow syndrome reveals abnormal neural gain but not neural noise. Brain 2022;24:1486–1498.

Donor Relations & Stewardship
Fundraising & Supporter Development, Virginia Woolf Building, 22 Kingsway,
London WC2B 6LE
stewardship@kcl.ac.uk